Analyzing perturbations in phyllotaxis of Arabidopsis thaliana

Yassin Refahi, Yann Guédon, Fabrice Besnard, Etienne Farcot, Christophe Godin, Teva Vernoux

Analyzing perturbations in phyllotaxis of *Arabidopsis thaliana*

Yassin Refahi[1], Yann Guédon[1], Fabrice Besnard[2], Etienne Farcot[1], Christophe Godin[1] and Teva Vernoux[2]

[1] CIRAD/INRA/INRIA, Virtual Plants INRIA team, UMR DAP, TA A-96/02,
34398 Montpellier Cedex 5, France
[2] Laboratoire Reproduction et Développement des Plantes, ENS/CNRS/INRA/Université Lyon I, 15 parvis
René Descartes - BP 7000, 69342 Lyon Cedex 07, France
Yassin.Refahi@sophia.inria.fr

Biological context

Vascular plants produce new organs at the tip of the stem in a very organized fashion. This patterning process occurs in small groups of stem cells, the so-called shoot apical meristems (SAM), and generates regular patterns called phyllotaxis. The phyllotaxis of the model plant *Arabidopsis thaliana* follows a Fibonacci spiral, the most frequent phyllotactic pattern found in nature. In this phyllotactic mode, single organs are initiated successively at a divergence angle from the previous organ close to 137.5°, the golden angle.

Cytokinins, a class of plant hormones, is involved in the control of phyllotaxis but its role has remained elusive (Vernoux *et al*., 2010). By analyzing the expression of several cytokinin signaling regulators in the meristem, we found that the pseudo-phosphotransfer protein AHP6 is expressed specifically during early organogenesis (unpublished results). AHP6 has been demonstrated to act as an inhibitor of cytokinin signaling (Mahonen *et al*., 2006) and we further observed a destabilization of phyllotaxis in *ahp6* null mutant. To understand how AHP6 acts in the control of *Arabidopsis* phyllotaxis, we analyzed sequences of divergence angles in both wild-type and *ahp6* mutant plants. We thus measured the divergence angle between successive flowers on a stem from the base (older flowers) to the top (younger flowers).
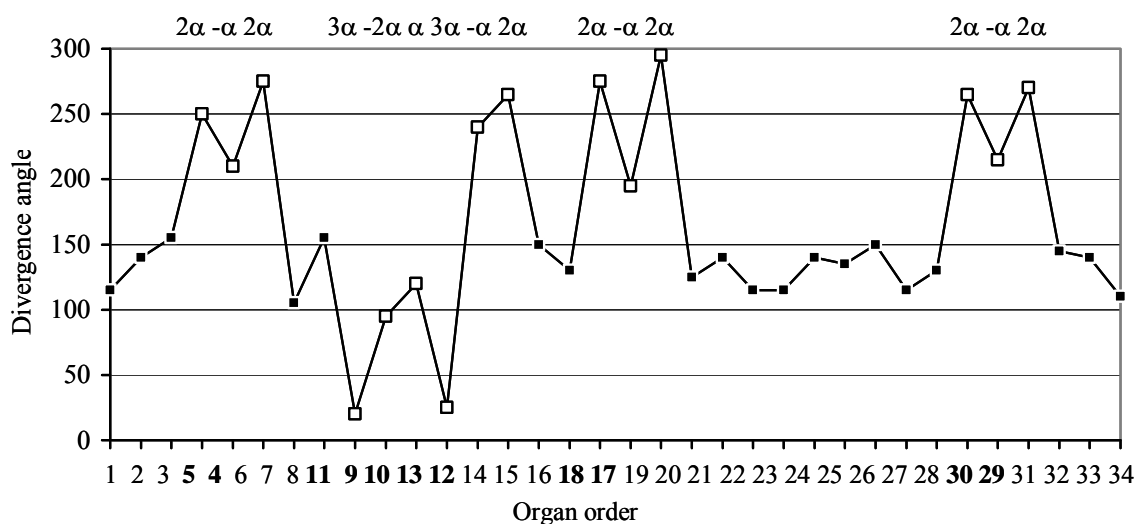
Modeling

The exploratory analysis highlighted two characteristics of the measured divergence angle sequences:
- Short segments (i.e. sub-sequences) of non-canonical divergence angles were identified along measured sequences (see an example in Figure 1) and were more frequent in the mutant.
- The measured divergence angles covered almost all the possible values (between 0 and 360) with highest frequencies around the canonical Fibonacci angle of $\alpha = 137.5°$. At least four classes of divergence angles were apparent but they were not unambiguously separated.

A motif corresponding approximately to $[2\alpha \ -\alpha \ 2\alpha]$ was frequently observed in wild-type and even more often in mutants. This motif can be simply explained by a permutation in the order of insertion on the stem (from the base to the top) of two consecutive organs, without changing the angle between them. This led us to hypothesize that the segments of non-canonical angles could be explained by permutations involving 2 or even 3 flowers (the most realistic numbers given the structure of the SAM).

To test this hypothesis, we designed a stepwise modeling approach with two objectives: (i) identify permutation patterns, (ii) optimally label the measured divergence angle sequences; see an illustration in Figure 1. In a first step, a hidden first-order Markov chain was estimated on the basis of the pooled wild-type + AHP6 measured divergence angle sequences. In this hidden first-order Markov chain, the states of the non-observable Markov chain represents "theoretical" divergence angles while the von Mises observation distributions attached to each state of the non-observable Markov chain represents measurement uncertainty.

The von Mises distribution, also known as the circular Gaussian distribution, is a univariate Gaussian-like periodic distribution for a variable $x \in [0, 2\pi)$. The von Mises observation distributions estimated for the five states of the non-observable Markov chain were centered on the multiples of the canonical divergence angle (-2α, -α, α, 2α, 3α). The optimally labeled divergence angle sequence (i.e. discrete sequence with five possible values chosen among -2α, -α, α, 2α, 3α) was then computed for each observed sequence using the estimated hidden first-order Markov chain. In a second step, the memories of a variable-order Markov chain were optimally selected (Csiszár and Talata, 2006) on the basis of these optimally labeled divergence angle sequences. This led us to identify frequent patterns corresponding to the permutation assumption: e.g. [2α -α 2α] corresponding to the organ order 1 3 2 4, [2α -α 3α -α 2α] corresponding to the organ order 1 3 2 5 4 6 (the divergence angle sequence is the first-order differenced organ sequence). This last pattern corresponds to two successive permutations. In a third step, a hidden variable-order Markov chain was estimated where the underlying variable-order Markov chain has the memories previously selected. The optimally labeled divergence angle sequence was then computed for each observed sequence using the estimated hidden variable-order Markov chain. The objective of this third step was to improve the quality of the labeling process both in terms of coverage of the observed sequence and posterior probabilities of the optimally labeled divergence angle sequences (i.e. weight of the optimally labeled divergence angle sequence among all the possible labeled divergence angle sequences that can explain a given observed sequence).

Figure 1: Example of AHP6 mutant divergence angle sequence with non-canonical labelled divergence angles and organ order deduced (permutations in bold).

The strength of this statistical modeling approach is the coherent probabilistic modeling used both for optimally labeling divergence angle sequences (with an associated quality indicator) and identifying permutation patterns. One shortcoming of this approach is that some multiples of the canonical divergence angle which occur rarely (e.g. 4α, 5α) as well as alternative phyllotaxis (e.g. Lucas with a canonical divergence angle of 99.5°) cannot be modeled. We thus chose to apply a mixed combinatorial/statistical model in order to further investigate these sequences. The proposed model can be seen as a latent structure model where the underlying Markov chain of the hidden Markov chain previously used is replaced by a combinatorial model that relies on the assumption that the permutation patterns are of length at most 3 (e.g. [3α -α -α 3α] corresponding to the organ order 1 4 3 2 5). Von Mises observation distributions centered on the multiples of the divergence angle were attached to the seven "states" (-α, -2α, α, 2α, 3α, 4α, 5α). The concentration parameter (inverse variance) common to the seven von Mises observation distributions was the concentration parameter estimated within the hidden Markov chain. The optimally labeled divergence angle sequence was then computed for each observed sequence using a lookahead algorithm.

These optimally labeled divergence angle sequences should be considered as more putative than the corresponding sequences computed using the hidden variable-order Markov chain due to the partial probabilistic modeling.

Results and discussion

The proposed modeling approach enabled to explain a large proportion of the non-canonical divergence angles despite the relatively high standard deviation (approx. 17°) of the estimated von Mises distributions. Wild-type plants were characterized by relatively frequent occurrences of 2-permutations generally isolated while *ahp6* mutants were characterized by the frequent occurrences of both 2- and 3-permutations whose succession generates highly complex motifs; see Table 1 and Figure 1.

Table 1: Optimally labeled divergence angle sequences. All the results are based on the mixed combinatorial/statistical model (CSM) except the % of unexplained angles which is also given for the hidden variable-order Markov chain (HMC). The Lucas phyllotaxis individuals contain long segments of organs following Lucas phyllotaxis.

	Wild-type plant	AHP6 mutant
No. sequences/No. organs	35/975	39/1098
% of non-canonical angles	20%	46%
% of unexplained angles	4% (HMC)/3% (CSM)	15%(HMC)/5%(CSM)
No. individuals, Lucas phyllotaxis	0	4
No. 2-permutations	64	120
No. 3-permutations	5	61

This work is the first large-scale analysis of *Arabidopsis* phyllotaxis and strongly supports our initial hypothesis by demonstrating that the order of insertion of consecutive organs on the stem can be affected without changing their relative angle. It reveals an intrinsic instability of the Fibonacci spiral phyllotaxis in wild-type plants due to these permutations. In most cases, the loss of *AHP6* activity strongly increased the frequency of these permutations, while the Fibonacci angle was maintained. This suggests that *AHP6* plays mainly a role in stabilizing the phyllotaxis by limiting the occurrence of the permutations. However, in a small number of plants, the loss of AHP6 leads also to a change in the phyllotaxis from a Fibonacci spiral to a Lucas spiral but showing similar instabilities. AHP6 could thus also play a more limited role in the definition of the divergence angle.

The expression of AHP6 during early organ initiation indicates that AHP6 likely exerts its role in phyllotaxis directly in the SAM. AHP6 could control the timing of emergence of consecutive organs and its loss would then result in permutations in the order of organ initiation in the SAM, explaining our observations. This hypothesis is currently under investigations. Finally, this modeling approach provides a new tool to investigate phyllotaxis and will pave the road for the identification of new genes controlling the patterning process of phyllotaxis. Moreover, it could help identifying other types of perturbations revealing new properties of phyllotaxis dynamics.

References

Csiszár I. and Talata Z. 2006. Context tree estimation for not necessarily finite memory processes, via BIC and MDL. *IEEE Transactions on Information Theory* 52, 1007-1016.

Mahonen A.P., Bishopp A., Higuchi M., Nieminen K.M., Kinoshita K., Tormakangas K., Ikeda Y., Oka A., Kakimoto T. and Helariutta Y. 2006. Cytokinin signaling and its inhibitor AHP6 regulate cell fate during vascular development. *Science* 311(5757), 94-98.

Vernoux T., Besnard F. and Traas J. 2010. Auxin at the Shoot Apical Meristem. *Cold Spring Harbor Perspectives in Biology*, published online.